The Self-assembly of Sepiolite and Silica Fillers for Advanced Rubber Materials: The Role of Collaborative Filler Network

Irene Tagliaro,[a] Elkid Cobani,[a] Elisa Carignani,[d] Lucia Conzatti,[b] Massimiliano D'Arienzo,[a] Luca Giannini,[c d] Francesca Martini,[d,e] Francesca Nardelli,[d] Roberto Scotti,[a] Paola Stagnaro,[b] Luciano Tadiello,[c] Barbara Di Credico[a,*]

[a] Dept. of Materials Science, INSTM, University of Milano-Bicocca, Via R. Cozzi, 55, 20125 Milano, Italy. Tel: +39-02-64485189; e-mail: barbara.dicredico@unimib.it

[b] Istituto di Scienze e Tecnologie Chimiche (SCITEC) "G. Natta", Consiglio Nazionale delle Ricerche (CNR), Via De Marini 6, 16149 Genova, Italy

[c] Pirelli Tyre SpA, Viale Sarca, 222, 20126 Milano, Italy

[d] Dipartimento di Chimica e Chimica Industriale, Università di Pisa, Via G. Moruzzi 13, 54126 Pisa, Italy

[e] Centro per l'Integrazione della Strumentazione Scientifica dell'Università di Pisa (CISUP), Lungarno Pacinotti 43, 56126, Pisa, Italy

Keywords: sepiolite, nanosilica, self-assembly, filler network, rubber nanocomposite.

Abstract

Composite materials based on hybrid filler systems can be a promising approach to produce advanced rubber nanocomposites (NCs). Recently, the positive effect of the combined use of silica

and sepiolite on NCs mechanical properties has been reported, compared to those of compounds reinforced with the same amount of the only silica filler. In this context, the present work aims at studying the possible synergistic self-assembly of nanosilica and sepiolite in the generation of a cooperative hybrid filler network in rubber-based NCs, in connection with material performance for tires application. In detail, the influence of the introduction of a secondary anisotropic filler in conjunction with isotropic nanosilica on their dispersion and interaction with the rubber matrix has been comprehensively investigated, in order to define the best formulation ensuring low rolling resistance and significant fuel saving.

NCs, containing simultaneously silica and sepiolite, either pristine (Sep) or chemically modified (mSep) by an acid treatment, were prepared by combining latex compounding (LCT) and melt blending techniques. Rheological and dynamic-mechanical analyses highlighted that the use of a double white filler, constituted by particles with different aspect ratio, affords a good balance between efficient reinforcement and low Payne effect.

TEM analysis evidenced the formation, within the rubber matrix, of cooperative superstructures due to the self-assembly of sepiolite and silica nanoparticles containing occluded rubber, when the secondary filler is mSep. The peculiar characteristics of mSep, characterized by fibers shorter than Sep and higher surface silanol bonding sites, bring about significant interactions between mSep and silica, which promote self-assembly of the two fillers in a collaborative hybrid network, improving dynamic-mechanical performances.

These results, even if related to sepiolite/silica NCs, demonstrate the effective role of the collaborative filler network, based on the hybrid double fillers, able to lend enhanced properties to rubber materials.

1. Introduction

Composite materials based on hybrid filler systems (Galimberti et al., 2017a), i.e. the combination of two or more type of fillers with different size and morphology, can be considered a promising alternative to conventional nanocomposites (NCs). Hybrid fillers can indeed improve the dispersion of each single filler in the polymer matrix which creates bridges among the particles, endowing an easier formation a percolative network, with remarkable benefits on the composite rheological properties (Galimberti et al., 2017a).

In the field of rubber-based NCs, the objective entailed in the use of hybrid fillers is to favor the nanoparticles self-assembly in a collaborative filler network (Scotti et al., 2014; Tadiello et al., 2015) involving the interactions of both fillers with the polymer matrix (Tripaldi et al., 2021), providing either higher polymer–filler interactions and tailored filler–filler interactions (Redaelli et al., 2018). It has been revealed that, besides the vulcanization process (Susanna et al., 2017; Mostoni et al., 2019), the fillers compatibility and the cooperative interactions at the nanoscale level lead to improved dynamic properties of rubber compounds, that is lower hysteresis at high temperatures, that imparts to tyres lower rolling resistance and, in perspective, lead to lower fuel consumption impacting on the transport costs (D'Arienzo et al., 2017).

For many years, the combination of silica and carbon black (CB) has been largely studied to exploit the advantages of both fillers in the rubber compounds. At first, the use of mixed fillers focused on the preparation of dual fillers based on a complex synthesis where silica particles are *in situ* generated in a CB matrix (Wang and Zhao, 2010). Successively, different authors (Feng et al., 2015; Senthilvel et al., 2016) demonstrated that the addition of small amounts of silica into CB rubber compounds decreases the filler cluster branching and increases the reinforcement efficiency, while higher silica loadings induce segregation phenomena, causing a deterioration in the filler–rubber interface and consequently in the rubber properties.

Based on this experimental evidence, tire industry has developed the use of hybrid filler systems, where CB is only partially substituted by precipitated silica functionalized with silane coupling

agents (Uhrlandt and Blume, 2001; Feng et al., 2015). These rubber compounds show improved dynamic response at low and high temperatures with respect to those reinforced solely with CB, which results in better rolling resistance and enhanced wet grip, while keeping satisfactory abrasion resistance. Also clay fillers, have been extensively investigated in combination with CB (Das et al., 2010; Galimberti et al., 2012), demonstrating that the anisotropic silica particles are critical to create a hybrid filler network in the presence of a nano-structured filler, such as CB, and revealing a significant affinity for the carbonaceous filler, prompting the enhancement of the filler networking phenomenon.

The above reported literature foreshadows that the improvement of mechanical properties in hybrid *filled composite materials* enclosing CB and silica is basically connected to the better dispersion of both fillers in the polymer matrix, which avoids the filler flocculation phenomenon (Mora-Barrantes et al., 2011). In the other words, the mixed reinforcing systems with CB reduce the entropic contribution, since the presence of fillers with different surface characteristics reduces their natural tendency to aggregate due to kinetic causes.

However, the behavior of rubber matrices reinforced with hybrid networks constituted exclusively by white fillers, has been rarely investigated. Bokobza et al., 2009 reported the effect of mixing organophilic sepiolite and silanized fumed silica on the mechanical behavior of styrene–butadiene rubber. In this case, a toluene dispersion of both fillers were added to a toluene solution of rubber. Final composites, containing 10 phr (parts per hundred rubber) of fillers, showed slightly enhanced properties compared to those of compounds reinforced with the same amount of the only silica filler. Nevertheless, the requirements of rubber matrix dissolution and low filler contents limits the extension of this methodology toward large scale applications.

Silica and modified montmorillonite were investigated as double fillers into natural rubber (NR) matrix, producing better stability of elastic modulus with temperature and an enhancement of stresses at all elongations (Galimberti et al., 2017b). The authors suggested a synergistic effect among fillers due to different aspect ratios (ARs) but, at last, they attributed the positive results to

the reduction of filler flocculation. Moreover, also in this case, the better performances are observed in the presence of low amount of anisotropic filler.

Actually, it is well known that anisotropic fillers improve the dynamic-mechanical behavior of the rubber NCs (Scotti et al., 2014; Tadiello et al., 2015) reducing the energy dissipation and, thus, the fuel consumption. This effect has been mainly ascribed to the formation of the nanoscale rigid rubber at the interface with the filler.

In view of these considerations, the clay/silica hybrid systems could be a possible strategy to further reduce the hysteresis of rubber materials, due to the potential synergistic effect between isotropic and anisotropic fillers in constituting a collaborative network. Actually, in the last decade, our group has focused the research activity on the use of sepiolite filler in rubber NCs to improve the mechanical properties of rubber materials (Giannini et al., 2016, 2018; Di Credico et al., 2018, 2019; Cobani et al., 2019; Tagliaro et al., 2020). In particular, we have recently reported on the preparation of polymer NCs based on nano-sized sepiolite fibers (Cobani et al., 2019), obtained by applying a controlled surface acid treatment on both pristine and organically-modified sepiolites. These nanosized Sep fibers, having reduced particle size and improved density of the surface silanol groups, provide, when embedded in rubber matrix, an excellent balance between reinforcing and hysteretic behavior, compared to the large-sized pristine Sep and isotropic silica. This has been attributed to the self-assembly of the anisotropic nanofibers in rigid filler network domains (Cobani, 2018; Cobani et al., 2019). Furthermore, nanosized sepiolite formulated with silica and CB in technical compositions for vulcanisable elastomeric materials produced a remarkable decrease of Payne effect and hysteresis while maintaining a good reinforcement of the elastomeric materials (Giannini et al., 2016; Di Credico et al., 2018; Tadiello et al., 2018).

Although several studies clearly showed that dual filler systems composed by silica and sepiolite positively impact on the properties of rubber composite (Bokobza, 2006; Locatelli et al., 2020; Staropoli et al., 2021), also in the presence of CB (Mohanty et al., 2021), to the best of our knowledge no work has yet systematically investigated the direct relationship between the synergic

interaction of different fillers in the network and the final material properties. Thus, there is a lack of studies which clearly demonstrate the occurrence of an effective cooperative filler network, with an interconnected structure of both clays and silica particles which experience direct interactions as well as their bridging by rubber chains.

In this context, the present work aims at exploring the possibility of a synergistic interaction between silica nanoparticles and different kinds of sepiolite fillers in the generation of a collaborative SiO_2/sepiolite hybrid network. In particular, the influence of the introduction of a secondary anisotropic filler in combination with isotropic silica on the filler dispersion and filler-rubber interactions will be further investigated, in order to attain a better tire performance in terms of lower rolling resistance and fuel saving.

Sepiolite fibers, previously modified with *N*-C14-18-alkyl-*N*,*N*-dimethylbenzylammonium (Sep), were selected to study the role of the organically modified Sep in promoting hybrid filler networking with silica. While the choice of this clay is tied to its good reinforcing properties, due to the high AR, the organic modifier is essential to enhance interfacial rubber/filler adhesion, considering the low compatibility between rubber and sepiolite, as already demonstrated inour previous study (Di Credico et al., 2018). On the other hand, although the organically-modified clays show better dispersion in a polymer matrix, the polymer-filler interaction is generally not improved because of the presence of hydrophilic silanol groups on the Sep surface. Along this line, the above mentioned Sep filler chemically modified by a controlled acid modification (mSep) was also investigated, since it presents an increased amount of surface silanols and decreased fiber size, which both favor the interfacial interactions with the polymer and the formation of filler network structure (Di Credico et al., 2018).

Rubber-based NCs containing silica and sepiolite were prepared by combining latex compounding technique (LCT) and melt blending. Highly filled NR masterbatches (MBs) were firstly prepared by coagulating NR latex and sepiolite aqueous suspension, as previously reported (Di Credico et al., 2019; Tagliaro et al., 2020). MBs were subsequently mixed with NR rubber matrix together with

150 silica filler, silane coupling agent, vulcanizing agents and antioxidants. This combined procedure is
151 convenient because it: i) improves the hydrophilic filler dispersion in the first stage, and ii) prevents
152 dust formation and filler loss during melt blending stage since the sepiolite fibers are previously
153 dispersed in NR MBs. Morphology, rheology and dynamic-mechanical properties of the achieved
154 NCs were compared with those of samples containing SiO_2, Sep, or mSep prepared by a traditional
155 melt blending procedure, in order to highlight the self-assembly effect of *hybrid filler systems* on
156 the final properties of the resulting materials. Moreover, the influence of the different fillers and of
157 the preparation techniques on the molecular mobility of NR in the NCs was investigated by ^1H
158 Time Domain Nuclear Magnetic Resonance (NMR).
159
160 **2. Experimental**
161 *2.1 Materials*
162 Sepiolite Pangel B5 (organically-modified with *N*-C14-18-alkyl-*N*,*N*-dimethylbenzylammonium,
163 Sep) was supplied by Tolsa and extracted from the landfill of Vallecas (Spain), while Silica Zeosil
164 MP1165 (BET specific surface area 160 m^2g^{-1} and average single particle dimension 22 nm) from
165 Solvay.
166 *Compounding of MBs and NCs*: NRL Medium Ammonia (MA) (60% w/w) was supplied by Von
167 Bundit. HCl (37% w/w) and NH_4OH (28-30% w/w) and isopropanol were purchased from Sigma-
168 Aldrich and used without any further purification.
169 NR is STR20 from Von Bundit; bis(3-triethoxysilylpropyl) tetrasulfide (TESPT) purchased from
170 Sigma-Aldrich; antioxidant *N*-(1,3-dimethylbutyl)-*N*-phenyl-*p*-phenylendiamine (6PPD), Santoflex-
171 6PPD; the curing agents were purchased as follows: Stearic acid (Stearina TP8) from Undesa;
172 sulfur from Zolfoindustria; zinc oxide (wurtzite, specific surface area 5 m^2 g^{-1}) from Zincol Ossidi;
173 *N*-cyclohexyl-2-benzothiazole sulfenamide (CBS) Vulkacit CZ/C from Lanxess. Milli-Q water with
174 a resistivity 18.2 MΩ cm was utilized.
175

2.2 Preparation of mSep by acid treatment

mSep was prepared according to a previously reported procedure (Giannini et al., 2018). 100 g of pristine Sep were dispersed in 1.5 L of deionized water and stirred at 70 °C (600 revolution per minute (rpm)). With an automatic pH-meter, 31 ml of aqueous 37% HCI were added over a period of 7 hours, at 70 °C, maintaining the pH around 3.0 ± 0.1. The resulting fibers were collected by centrifugation and the powders were washed several times with deionized water and aqueous ammonium hydroxide (60%) in order to remove chloride anions, until pH 7± 0.2. Finally, the obtained solid was dried in an oven at 100 °C for 48 h. From the X-ray fluorescence (XRF) analysis of mSep samples, 35% by weight of magnesium resulted extracted (data previously reported in Tadiello et al., 2018).

2.3. Preparation of MBs

Sep MB samples containing high amounts of filler were prepared according to a previously reported procedure (Di Credico et al., 2019).

10 g of Sep (Sep or mSep) was dispersed in water (500 mL), sonicated for 30 min and then mixed with a mechanical stirrer (Velp Scientifica Stirrer DLS) at 500 rpm. In another vessel, 16.7 g of NRL-MA (corresponding to 10 g of dried NR) were diluted with 125 ml of distilled water and stirred for 10 min at 100 rpm. Then, the diluted NRL solution was slowly poured into the previous Sep dispersion, under stirring at 500 rpm until the flocculation of the Sep MBs (MB-Sep or MB-mSep) was completed (30 s). Sep MBs were separated from the liquid phase through filtration, washed with water to remove ammonium residuals, and portioned in small pieces. MB samples were dried under nitrogen at 10-2 bar at 80 °C for 48 h.

2.4 Preparation of NCs

The composite materials were prepared incorporating MBs to NR matrix and other compounding ingredients in a Brabender Plasti-Corder lab station internal mixer (65 mL mixing chamber, 0.6 filling factor) through thermomechanical blending.

The production of NC materials consists of three mixing steps. Times and temperatures were selected according to the thermal stability of the reactants and to the workability of rubber. The amount of filler (SiO_2 or SiO_2/Sep) was kept constant at 32 phr. In the first step, NR was masticated at 120 °C and 60 rpm rotor speed for 30 s. Then, filler or MB were added together with TESPT (2.5 phr) to the masticated rubber in three subsequent aliquots and mixed. After two minutes of mixing, 6PPD (2 phr), zinc oxide (3.5 phr) and stearic acid (2 phr) were then added and masticated for further 5 min. In the second step, the obtained compounds were reloaded in the mixing chamber and masticated at 90 °C and 60 rpm for 3 min; sulfur (1 phr) and CBS (3 phr) were then added and mixed for further 2 min. In the third step, the resultant materials were processed in a two-rolling mill at 50 °C for 3 min for improving their homogeneity. Reference materials containing Silica Zeosil 1165 (Solvay), Sep and mSep were prepared by this procedure.

Vulcanization process was performed in a hydraulic press at 170 °C and 100 bar for 10 min.

Cured composite materials, compounded starting from Sep and mSep are named Sep+SiO_2/NR and mSep+SiO_2/NR, respectively; analogously, those compounded starting from MBs are called MB-Sep+SiO_2/NR and MB-mSep+SiO_2/NR, respectively. Cured reference material, containing only silica filler is labelled as SiO_2/NR. The compositions of the NCs are summarized in Table 1.

2.5 Morphological characterization of cured NCs

50 nm thick sections of all vulcanized composite materials were cut by a Leica EM FCS cryo-ultramicrotome, equipped with a diamond knife, by keeping the samples frozen at −130 °C. The morphology of vulcanized compounds was investigated at different magnifications by TEM analysis with a Zeiss EM 900 microscope (80 kV).

Table 1 Filler formulations of composite materials*

Sample	SiO_2	Sep	mSep	TESPT	Stearic acid	6PPD	ZnO	CBS	S
SiO_2/NR	32	-	-	2.5	2	2	3.5	3	1
Sep+SiO_2/NR	16	16	-	2.5	2	2	3.5	3	1
MB-Sep+SiO_2/NR	16	16	-	2.5	2	2	3.5	3	1
mSep+SiO_2/NR	16	-	16	2.5	2	2	3.5	3	1
MB-mSep+SiO_2/NR	16	-	16	2.5	2	2	3.5	3	1

* Amount of ingredients expressed in phr (parts per hundred rubber)

2.6 Dynamic-mechanical analysis composites

Uncured materials were cut by using a Constant Volume Rubber Sample Cutter (CUTTER 2000, Alpha Technologies) obtaining samples of 3.5 cm diameter, ≈ 0.2 cm thickness and 6 ± 0.3 g.

Curing was performed with a Rubber Process Analyzer (RPA2000, Alpha Technologies) under the following conditions: oscillation angle ± 1°, 170 °C, 15.65 kPa for 10 min (time sufficient to reach the curing plateau). The following parameters were obtained: M_L is the minimum torque measured, M_H is the maximum torque measured, and the scorch time is the time needed to start the vulcanization process.

After curing, vulcanized samples were analyzed by dynamic-mechanical measurements with the same instrument applying a shear stress mode. Strain sweep experiments (0-10% strain) were carried out at 70°C and 10 Hz. Five measurements were performed for each sample, and the average value was reported.

The storage modulus (G′) at different strain values was evaluated and discussed. To better understand the variation in mechanical properties due to double hybrid fillers with respect to

standard nanosilica, we report the values of G'at 0,5% as G'_0 and G' at 10% as G'_∞ in order to evaluate the reinforcement, Payne effect and hysteresis of rubber materials.

2.7 ^1H Time Domain NMR

^{1}H Time Domain NMR measurements were performed at a Larmor frequency of 20.8 MHz using a Niumag permanent magnet interfaced with a Stelar PC-NMR console. A 5 mm probe was used with a ^{1}H 90° pulse duration of τ_{90} = 3 μs for all samples. On-resonance Free Induction Decays (FIDs) were recorded for all samples and standard samples using the Magic Sandwich Echo (MSE) pulse sequence (Rhim et al., 1971; Matsui, 1991) with a total echo duration of $\tau_{MSE} = 6\ (4\tau_\varphi + 2\tau_{90}) = 72$ μs, with τ_φ = 1.5 μs, using a dwell time of 0.1 μs and 8k acquisition points; 300-800 scans were accumulated using a recycle delay of 5 times the measured ^{1}H T_1 (3-10 s), in order to guarantee quantitative measurements. For all composite materials and for pure compounds displaying a slowly decaying component of the FID (NR and SiO_2), Carr-Purcell-Meiboom-Gill (CPMG) sequence (Meiboom and Gill, 1958) was also acquired; 400 transients were accumulated acquiring 2000 data points. For the construction of MSE/CPMG relaxation curves, the first 180 data points of the MSE ^{1}H FID (recorded within the first 180 μs of the acquisition) were joined together with all the data points of the CPMG experiment recorded after 180 μs of acquisition. In order to eliminate residual water which could alter the results of the ^{1}H FID analysis of isolated components, Sep and SiO_2 samples were dried in an oven at 105 °C for 16 hours before acquisition.

The experimental MSE ^{1}H FID's or the combined MSE/CPMG relaxation curves were analyzed by a discrete approach using a non-linear least square fitting procedure implemented in the Mathematica® environment (Wolfram Research Europe Ltd, Oxfordshire, United Kingdom).

3. Results and Discussion

Combined latex and melt blending compounding techniques were applied for preparing *hybrid filled composite materials* containing both silica and sepiolite (Table 1).

Highly loaded MBs containing Sep or mSep were firstly prepared by co-coagulation of NR latex and filler dispersions by LCT approach, in order to take advantage of good dispersion of both Sep and mSep fillers in aqueous medium. In fact, since the Sep dispersion shows a positive zeta potential, ascribable to the presence of the alkylammonium salt (Di Credico et al., 2019), this gives rise to the fillers repulsion especially at high Sep concentration, favoring an efficient and stable colloidal dispersion. This occurs also for mSep, where the ammonium salt is only partially removed during acid treatment. In addition, mSep benefits also the enhanced hydrophilic silanol groups onto filler surface.

In the subsequent step, MBs were compounded by melt blending with the NR rubber matrix and silica filler together with silane, coupling agent, vulcanizing agents, and antioxidants.

The combined latex/melt blending approach is a valuable procedure for several reasons: i) hydrophilic filler dispersion is improved; ii) filler loss during processing is reduced in case of compounding filler with low bulk density, like Sep; iii) abrasion and scratching on blending machines are inhibited, because the fillers are previously dispersed in NR MBs; iv) high processing temperatures are avoided, since severe friction phenomena among filler particles are hindered.

A critical evaluation of the effect of hybrid filler systems on rheological and mechanical properties of final NC materials was performed, considering as a reference a compound with silica as single filler. In addition, the features of hybrid filler compounds obtained by the combined techniques (MB-Sep+SiO_2/NR, MB-mSep+SiO_2/NR) were compared to those of NCs prepared by traditional compounding (Sep+SiO_2/NR, mSep+SiO_2/NR), where both fillers were introduced by melt blending.

The rheometric characteristics of hybrid filled NCs, expressed in terms of the minimum torque (M_L) and the maximum torque (M_H), are reported in Table 2.

The scorch time, defined as the time needed for the vulcanization to start, is a crucial parameter for the industrial moulding of the material (Susanna et al., 2017). As reported in Table 2, the scorch time of all the samples varies in the range of 2.0 – 2.5 min. In particular, the scorch times of silica-

filled NR compounds with organoclay as co-fillers are slightly lower compared to the reference compound with silica alone. It is well known that free silanol groups on the silica surface interfere with the vulcanization process due to their acidic nature and their tendency to adsorb accelerators, thus retarding the vulcanization. In the case of the hybrid filler systems, the use of organoclays having a quaternary ammonium modifying agent protects the silanols groups decreasing the scorch time as reported by other authors (Sattayanurak et al., 2019). However, both Sep+SiO_2/NR and mSep+SiO_2/NR, the scorch time only slightly decreased and thus in line with the standard time required in the rubber industry.

Table 2 Curing characteristic of rubber NCs.

	Scorch time (min)	M_L (dNm)	M_H (dNm)	M_H-M_L (dNm)
SiO_2/NR	2.5 (±0.2)	2.3 (±0.1)	15.8 (±0.2)	13.5 (±0.3)
Sep+SiO_2/NR	2.0 (±0.2)	2.0 (±0.1)	13.5 (±0.2)	11.5 (±0.3)
MB-Sep+SiO_2/NR	2.0 (±0.2)	2.1 (±0.2)	12.3 (±0.2)	10.2 (±0.4)
mSep+SiO_2/NR	2.3 (±0.2)	2.1 (±0.1)	12.9 (±0.3)	10.8 (±0.4)
MB-mSep+SiO_2/NR	2.0 (±0.2)	1.7 (±0.2)	11.6 (±0.2)	9.9 (±0.4)

Moreover, considering the high adsorption properties of these clay minerals, the comparable scorch times observed in all the samples is a proof of similar vulcanizing agent adsorption on both sepiolite and standard silica.

The minimum torque (M_L), which is the torque at the initial stage of the vulcanization process, can be considered a parameter related to viscosity. Generally, the samples containing sepiolite show slightly lower M_L compared to those containing silica alone. This could be related to free ammonium salt, contained in both nanofillers, which can act as lubricant and secondary accelerator of vulcanization (Di Credico et al., 2018).

At the same time, the lowest value of M_L of MB-mSep+SiO_2/NR could be attributed to the better dispersion of filler mSep, having high amount of silanols after acid modification, by using LCT, providing lower viscosity in the final NC.

The presence of hybrid filler systems in NR matrix gives satisfactory values of the maximum torque (M_H), which is a measure of the crosslink density and stiffness of the rubber, including also the contribution of filler-network. In detail, the organoclay-containing compounds show a small decrease in M_H and torque increment (which is the M_H-M_L), which may be again related to the effect of the modifying agent of the organoclay and the desired decrease in filler networking. On the other hand, it is noteworthy that the decrease of M_H value is almost irrelevant, especially in comparison to the results recently reported by other authors (Sattayanurak et al., 2019), where a considerable decrease in torque is observed even with the addition of small amounts of secondary organoclay filler. Also, M_H value of the samples formulated by MB is not significantly influenced by the combined compounding technique, proving the maintenance of the material properties. This suggests that the material formulated by LCT was not corrupted by possible oxidation processes, found in other cases during aqueous flocculation process in the presence of sepiolite (Carignani et al., 2020). The high M_H-M_L value found for the SiO_2/NR sample confirms the excellent interaction with the sulfur-based vulcanization compounds. With respect to this sample, the NCs containing sepiolite show values slightly lower of about 2 dNm.

The impact of secondary filler on the mechanical properties of hybrid filled composites was studied also by monitoring the dependence of the storage modulus (G') on the strain. The curves in Fig. 1 show: i) higher modulus at low strain (G'_0) value of SiO_2/NR (black line); ii) higher G'_0 and modulus at high strain (G'_∞) values for the composites obtained by traditional melt blending with respect to those obtained by MB; iii) $\Delta(G'_\infty–G'_0)$ values much lower in the samples containing both mSep and SiO_2, independently on the preparation method (red and red dotted lines).

Table 3 reports dynamic parameters, *i.e.* the storage modulus G'_0, the Payne effect $\Delta(G'_0$-$G'_\infty)$ and loss factor as TanDelta (9%). G_0' represents the filler-filler interaction and thus the measure of filler

reinforcement, while the so-called Payne effect is caused by the hysteretic breakdown at small strains of the filler network derived by fillers joined together or through polymer layers. During deformation, the hysteretic breakdown and reformation of the network is associated with the energy dissipative process. In tires, this energy loss is the major contribution to the rolling resistance and represents an undesirable effect, determining a high fuel consumption.(Cobani et al., 2019) In this regard, TanDelta (9%) can be considered a good parameter for hysteresis estimation in vulcanized rubber and thus an indication of the rolling resistance contribution of the compound (D'Arienzo et al., 2018; Scotti et al., 2018).

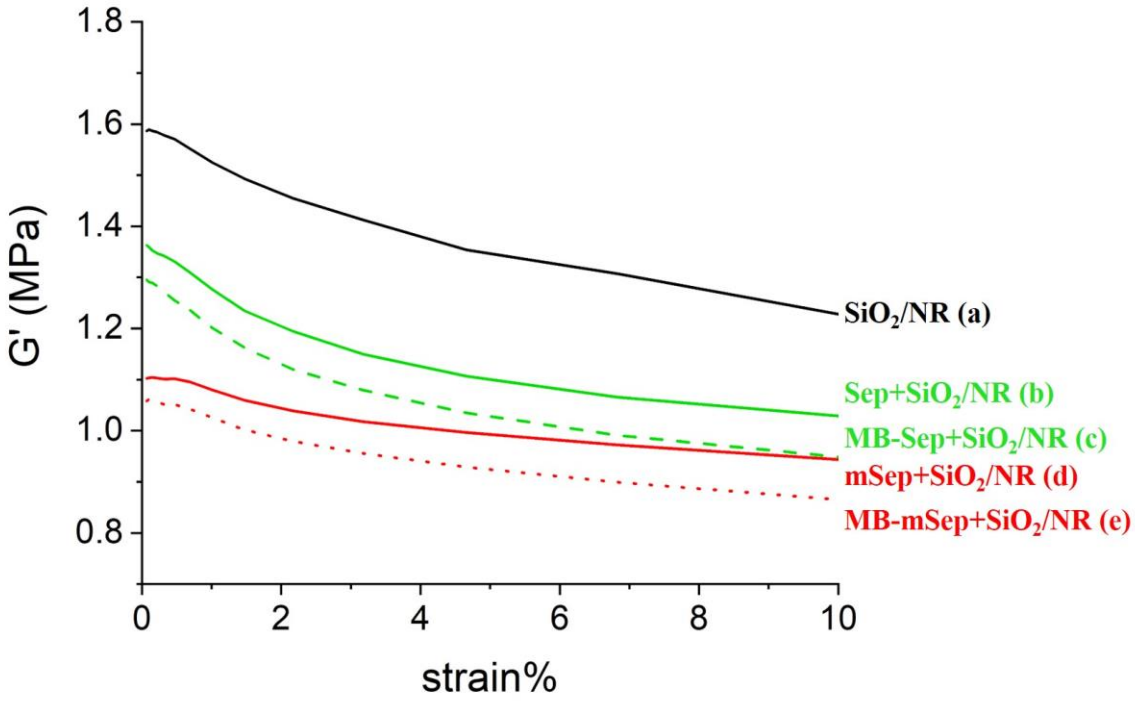

Fig. 1 Loss modulus G′ *vs* strain of SiO_2/NR (a, black line), Sep+SiO_2/NR (b, green line), MB-Sep+SiO_2/NR (c, green dashed line), mSep+SiO_2/NR (d, red line), MB-mSep+SiO_2/NR (e, red dotted line).

Table 3 Dynamic properties: storage modulus at low strain G'_0, Payne effect as $\Delta(G'_0-G'_\infty)$, loss factor as TanDelta (9%) of cured samples. Lettering refers to Fig.1.

	G'_0 (MPa)	**$\Delta(G'_0-G'_\infty)$ (MPa)**	**TanDelta (9%)***
SiO_2/NR (a)	1.25 (± 0.05)	0.34 (± 0.02)	0.07 (± 0.01)
Sep+SiO_2/NR (b)	1.04 (± 0.05)	0.30 (± 0.02)	0.06 (± 0.01)
MB-Sep+SiO_2/NR (c)	0.96 (± 0.05)	0.30 (± 0.02)	0.07 (± 0.01)
mSep+SiO_2/NR (d)	0.95 (± 0.05)	0.16 (± 0.02)	0.05 (± 0.01)
MB-mSep+SiO_2/NR (e)	0.88 (± 0.05)	0.19 (± 0.02)	0.07 (± 0.01)

***Calculated as ratio of the G' and storage modulus (G") at 9 % of strain.

SiO_2/NR sample shows the highest G'_0 value, suggesting a remarkable interaction among filler particles. The presence of double fillers produces only a slight decrease in the reinforcement, which remains in the same range of that of SiO_2/NR composite.

Interestingly, the Payne effect of NCs containing both silica and sepiolite is reduced with respect to that containing only commercial silica (SiO_2/NR sample). In particular, samples with mSep, *i.e.* mSep+SiO_2/NR and MB-mSep+SiO_2/NR, display significantly low Payne effect values.

In addition, the dynamic loss tangent in mSep+SiO_2/NR is reduced (0.05) compared to composites including both silica alone (0.07) and untreated Sep (0.06), suggesting that double fillers promote the filler-rubber interactions, particularly when Sep is modified by acid treatment (mSep). This is supported also by lower values of the loss modulus (Fig. S1) for mSep+SiO_2/NR and MB-mSep+SiO_2/NR, at small and high strains, indicating a significant reduction of the energy dissipation during deformation, and the improvement of breakage and rebuilding of filler-filler network and slippage of the polymer chains.

The TanDelta values of NCs prepared by MB result higher than those prepared with traditional melt blending compounding. This could be related to poorer interdiffusion of the two filler networks, and in a lower effect of the presence of nanoclays, resulting in a lower suppression of the silica self-interacting forces (filler-filler interactions). This is also justified by the lower shear forces developed during the mixing when using a MB approach.

Thus, the use of hybrid filler systems, especially those based on mSep and SiO_2, appears promising, since they produce a remarkable reduction of Payne effect and rolling resistance, without originating negative effects on the reinforcement. This peculiar behaviour envisages a favourable compatibility between mSep and SiO_2 fillers and, in turn, the formation of an effective collaborative network at the nanoscale level.

To support this hypothesis, double filled NCs were investigated by TEM analysis and morphological observations were correlated to the dynamic-mechanical data. TEM images of Sep+SiO_2/NR, MB-Sep+SiO_2/NR, mSep+SiO_2/NR and MB-mSep+SiO_2/NR samples are reported in Fig. 2 and 3. The analysis carried out at different magnifications reveals a rather complex spatial distribution of both silica nanoparticles and sepiolite fibers, which relies on both the NC preparation method and the sepiolite kind.

In the Sep+SiO_2/NR sample (Fig. 2a,a'), the distribution of both fillers appears fairly homogeneous. At low magnification (images not shown), large agglomerations with elongated shapes, generally oriented in one direction and constituted by only Sep fibers or silica particles are detectable; among them, silica aggregates, sub-micrometric Sep bundles, and isolated fibers are also found at higher magnification (Fig. 2a'). The observed morphology does not highlight any specific interaction between spherical SiO_2 particles and Sep fibers, and supports the similarity of G' and TanDelta values of this sample to those of SiO_2/NR.

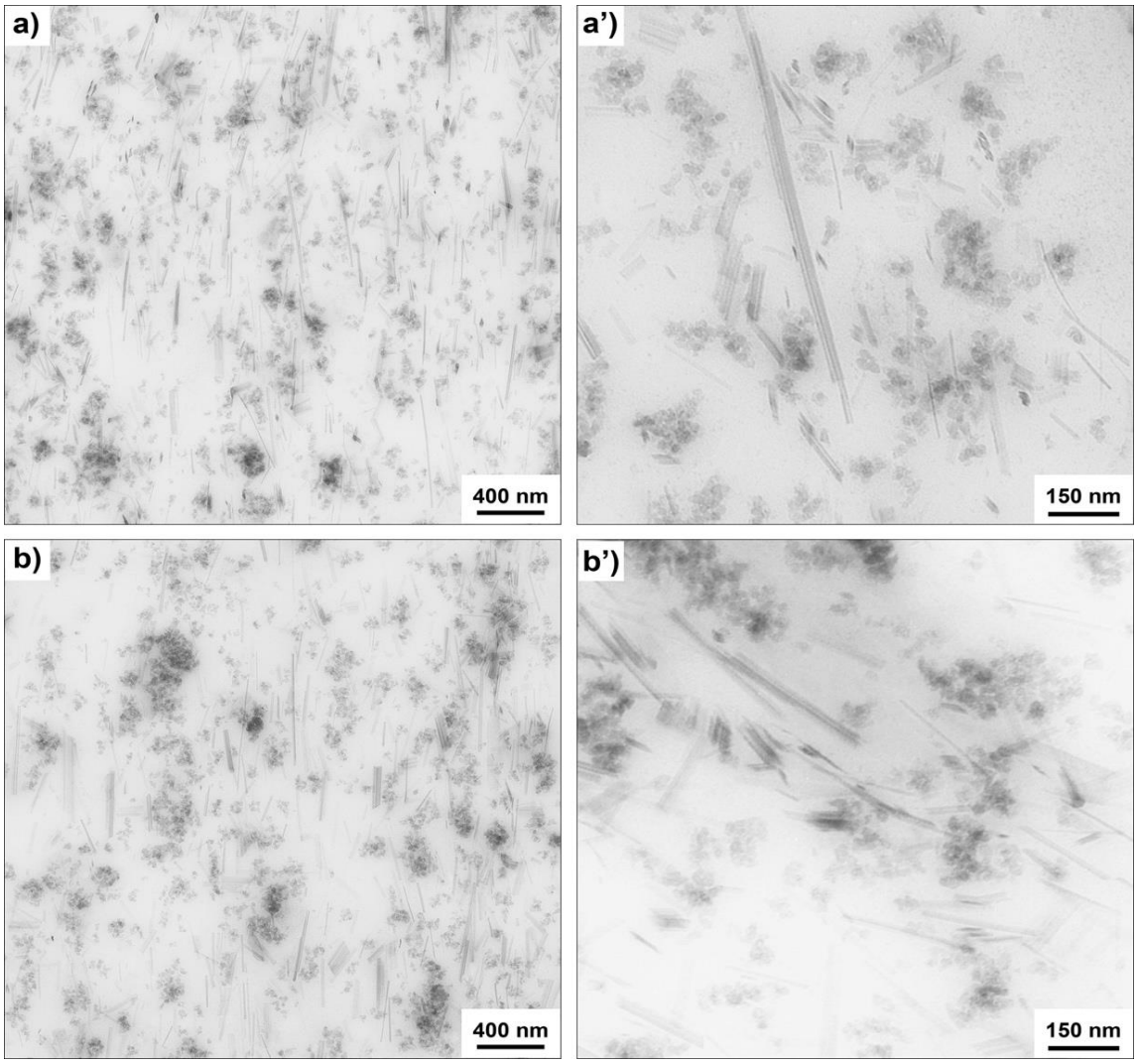

Fig. 2 TEM images at different magnifications of (a, a') Sep+SiO_2/NR and (b, b') MB-Sep+SiO_2/NR samples.

The preparation method involving the pre-dispersion of Sep in the MB (MB-Sep+SiO_2/NR sample) results in composites where a slightly less homogenous and finer distribution of the organoclays is detectable (Fig. 2b). Large filler agglomerations are not observed at low magnification (images not shown), but only sub-micrometric silica aggregates and Sep bundles, together with numerous isolated Sep needles. The hybrid filler networking does not appear continuous and homogeneous for the presence of self-assembled Sep domains with occluded rubber and partially oriented fibers (Di

406 Credico et al., 2018); moreover, any particular affinity between the two fillers is observed at higher
407 magnifications (Fig. 2b').
408 TEM images of NCs prepared with mSep and SiO_2 hybrid filler (Fig. 3) show a significantly
409 different morphology compared to of composites containing untreated Sep (Fig. 2). In
410 mSep+SiO_2/NR sample, obtained by traditional melt blending, both mSep bundles and silica
411 aggregates of elongated shapes (2 - 5 μm length) and preferentially aligned in one direction are
412 found at low magnification (images not shown). The presence of a larger number of micrometric
413 bundles (as those shown in Fig. 3a) suggests interactions between the fibers higher than those
414 observed for Sep, probably due to the high number of surface silanol sites and the reduced particles
415 size (Di Credico et al., 2018) of these treated fibers. A high number of isolated Sep needles and
416 superstructures of sub- or micrometric dimensions, composed by sepiolite fibers and silica
417 nanoparticles connected by thin polymer films, are noticeable at higher magnification (Fig. 3a').
418 These morphological features seem to support the existence of a cooperative hybrid filler network.
419 The morphology observed in the MB-mSep+SiO_2/NR sample (Fig. 3b,b'), which is characterized
420 by a fine mSep dispersion with a relevant number of isolated Sep needles and sub-micrometric
421 superstructures (Fig. 3b') similar to those observed in the mSep+SiO_2/NR sample (Fig. 3a'), further
422 endorse these considerations/hypothesis. Also, in this case, the mSep particles in the superstructures
423 appeared preferentially aligned in one direction and the affinity between fibers and silica aggregates
424 is in line with the reduced Payne effect and hysteresis previously discussed.

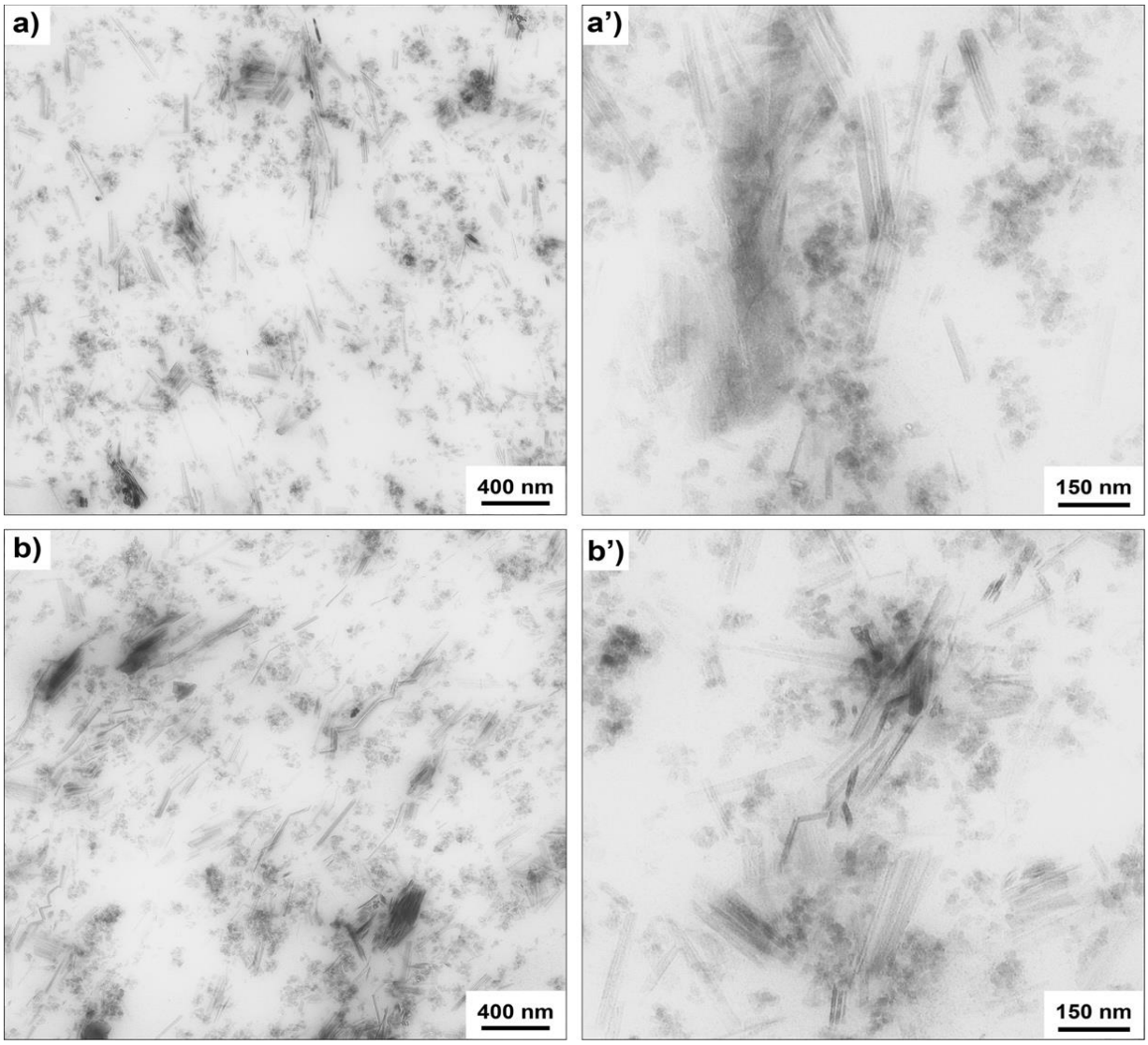

Fig. 3 TEM images at different magnifications of (a, a') mSep+SiO_2/NR and (b, b') MB-mSep+SiO_2/NR samples.

Moreover, both filler distribution and dispersion result improved with respect to those of the sample obtained with the traditional procedure, as already observed for the hybrid NCs containing Sep.

In summary, the morphological survey suggest the formation, within the rubber matrix, of cooperative superstructures due to the self-assembly of sepiolite and silica nanoparticles containing occluded rubber, when the secondary filler is mSep, which is obtained by a controlled acid treatment and is characterized by shorter fibers and higher surface silanol bonding sites (Di Credico et al., 2018). These peculiar characteristics of mSep bring about significant interactions between

mSep and silica, which result in a promoted self-assembly of the two fillers in a collaborative hybrid network, improving dynamic-mechanical performances and, in particular, significantly reducing the Payne effect.

The influence of the simultaneous presence of two different filler systems and of the preparation techniques on the dynamic properties of the NCs at a molecular level, was studied by low-resolution solid state NMR techniques, which exploit the measurement of ^1H T_2 relaxation times to distinguish and quantify protons belonging to environments with different molecular mobility.

In particular, on resonance FID and CPMG decays were acquired for double filled NCs and for all the pure components present in the formulations, by combining MSE and CPMG experiments (three examples are shown in Fig. 4a). The MSE pulse sequence was exploited to refocus the short decaying signal deriving from protons in rigid environments. On the other hand, the CPMG sequence was used to measure ^1H T_2 associated with the slow-decaying components of the ^1H signals, which in a free decay can be shortened by non-dynamics contributions, such as the magnetic susceptibility of the sample and/or fluctuations of the external magnetic field.

For all the double filled NCs, the combined MSE/CPMG relaxation curves are well reproduced by fitting a linear combination of three different functions (the case of MB-mSep+SiO_2/NR is shown in Fig. 4b), each characterized by a T_2 (T_2^i) and a weight percentage (W^i%). Specifically, one Gaussian function (gau) and two exponential functions (exp1, exp2) were used to reproduce the decays associated to protons in rigid (T_2 = 10-50 μs), intermediate (T_2 = 50-1000 μs) or mobile (T_2 > 1 ms) environments, respectively. The fitting of MSE/CPMG relaxation curves allows to quantify the three domains with different mobility and to determine all the T_2 values (Table 4). At a first inspection, we can observe a similar behavior of all double filled NCs with a predominant domain of mobile protons (66-67%) with T_2 of about 5 and 6 ms for vulcanized and crude samples, respectively; a 23-25% of protons display an intermediate mobility and only 8-11% of protons result in a rigid environment.

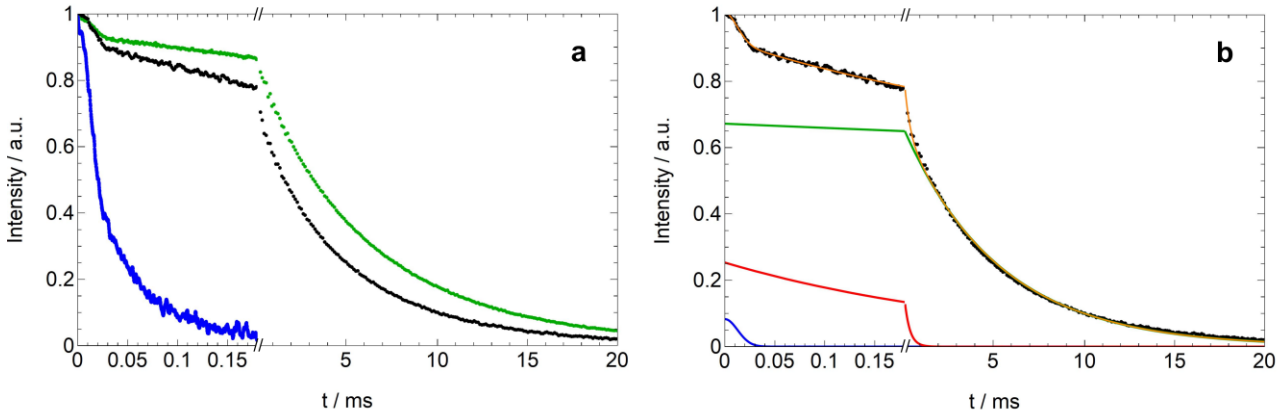

460

461 **Fig. 4** (a) ^{1}H MSE FID of mSep (blue) and combined MSE/CPMG relaxation curves of NR (green)
462 and vulcanized MB-mSep+SiO_2/NR (black). (b) Experimental (black) and best-fit (orange line)
463 MSE/CPMG relaxation curve of vulcanized MB-mSep+SiO_2/NR. Together with the total fitting
464 function (orange line) and the single contributions of the Gaussian (blue line), intermediate-T_2 (red
465 line), and long-T_2 (green line) exponential functions are shown.

466 To get quantitative information on the molecular mobility of NR in connection with the fillers
467 network, we performed an analysis by comparing the weights obtained from the fitting of the
468 experimental curves and the theoretical weights, which were calculated under the assumption that
469 all the components maintain the degree of mobility of their pure state also in the NCs.
470 Practically, the theoretical evaluation was done in several steps, which include the experimental
471 determination of the hydrogen content for all the pure components by construction of a calibration
472 curve with standard solid compounds (technical details on the calculations are reported in SI; a
473 similar procedure for the estimation of the proton content in the pristine materials was already
474 reported (D'Arienzo et al., 2018). By exploiting the MSE experiment, the percentage of hydrogen
475 deriving from each pure compound on the total hydrogen content in the NCs was calculated; then,
476 based on MSE FID's or combined MSE/CPMG relaxation curves, the weights of protons in rigid,
477 intermediate and mobile fraction were determined for each pure compound. By combining these
478 results, the theoretical weights of protons in rigid, intermediate and mobile fraction for the NCs

were evaluated (Table 4). To notice, since Sep+SiO_2/NR and MB-Sep+SiO_2/NR (and mSep+SiO_2/NR and MB-mSep+SiO_2/NR) contain the same amounts of pure compounds, their theoretical evaluation results identical. The calculation of the theoretical weights does not take into account possible changes of molecular mobility induced by the physical interactions between the materials present in the composite, such as rubber-filler interactions, which may also differ depending on the type of procedure used to prepare the composites.

Therefore, in order to unveil such plausible changes, the theoretical results obtained for Sep+SiO_2/NR and on mSep+SiO_2/NR samples (equal to those for the corresponding samples prepared by LCT) have been compared with the T_2 analysis of the MSE/CPMG relaxation curves obtained for NC samples prepared through the formation of MBs or by traditional melt blending (Table 4). From the comparison of the theoretical estimates and the analyses of the real composites, several differences can be observed, the most relevant being that real samples, containing both spherical and anisotropic fillers, show larger weights of the domain with intermediate mobility, associated with smaller percentage of protons in very mobile domains. It is also worth noting that such difference (about 5-8%), even if not very big, is reproducible in all hybrid filler NCs and might be explained with the formation of a loosely-bound rubber, displaying a T_2 of about 200-250 μs. Indeed, in the literature values of T_2 of the order of 10–20 μs have been associated to "tightly bound rubber" (i.e., chains experiencing a very restricted overall mobility), as distinguished from "loosely bound rubber", experiencing a larger degree of mobility and associated to ^{1}H T_2 values of the order of several tens/hundreds of μs (O'Brien et al., 1976; Ou et al., 1996; Borsacchi et al., 2018).

It is worth noting that, in the case of crude samples, the percentage of protons in rigid environments remains almost the same compared to the theoretical evaluation; conversely, for the vulcanized sample the weight of the rigid component is slightly lower. This might be caused by the presence of crystalline compounds in the crude samples, which may react or melt during vulcanization.

Table 4. Results of the analysis of the MSE/CPMG ^{1}H FIDs* recorded for both crude and vulcanized composite samples, and theoretical weights obtained as described in the text.

	Gau	Exp1	Exp2
	W^1% (T_2^1/μs)	**W^2% (T_2^2/μs)**	**W^3% (T_2^3/ms)**
Sep+SiO_2/NR crude	11 (16)	23 (212)	66 (6.4)
MB-Sep+SiO_2/NR crude	10 (16)	24 (208)	66 (6.2)
mSep+SiO_2/NR crude	11 (17)	22 (266)	67 (6.2)
MB-mSep+SiO_2/NR crude	10 (17)	23 (254)	67 (6.2)
Sep+SiO_2/NR	8 (15)	25 (170)	67 (5.2)
MB-Sep+SiO_2/NR	8 (16)	25 (215)	67 (5.3)
mSep+SiO_2/NR	9 (16)	25 (258)	66 (5.2)
MB-mSep+SiO_2/NR	9 (17)	25 (280)	66 (5.2)
Theoretical for Sep+SiO_2/NR and MB-Sep+SiO_2/NR	11	17	71
Theoretical for mSep+SiO_2/NR and MB-mSep+SiO_2/NR	11	17	71

*The values of ^{1}H T_2 relaxation times obtained for each of the three functions (Gau, Exp1, Exp2) used to fit the MSE/CPMG relaxation curves are reported in brakets and expressed in μs (or ms in the case of Exp2).

Importantly, the different procedures used to prepare the composites did not significantly affect the distribution of the domains with different mobility, evidencing the fact that the LCT has a similar effect on proton dynamics in the final product compared to melt blending.

Thus, NMR measurements indicate the formation of a noticeable fraction of loosely bound rubber in hybrid filled NCs, even if do not highlight significant differences among samples prepared with Sep or mSep. This can be related to the fact that ^{1}H T_2 are sensitive to very local nuclear environments and therefore only probe short range interactions (on sub-nanometric scale). In other words, it is plausible that short range interactions are very similar for Sep and mSep, while

rheological and mechanical behaviour can be more influenced by longer range morphologies (on a hundred of nanometres scale), which result different for NCs containing treated and untreated Sep, as evidenced by TEM images.

4. Conclusions

Rubber-based NCs containing silica and sepiolite were prepared by combining LCT and melt blending processes, with the aim of evaluating the effect of the self-assembly of hybrid fillers (silica/sepiolite) and of the combined preparation technique on the final materials properties.

A critical evaluation of rheological and mechanical properties of final hybrid filled NC highlights that: i) the combined procedure is a simple and effective method to obtain high-performance rubber NCs; ii) the use of double white fillers, having different aspect ratios, allows to obtain a good trade-off between efficient reinforcement and low Payne effect, in particular when the secondary filler is mSep. Morphological TEM analysis suggests that this result may be associated with the formation of cooperative fillers network based on the synergic interaction of both sepiolite and silica nanoparticles with the polymer matrix, providing a higher polymer–filler interactions. In agreement with this hypothesis, ^{1}H Time Domain NMR experiments indicate the formation of a noticeable fraction of loosely bound rubber in hybrid filled NCs.

This study, even if referred to Sep/SiO_2 double fillers, provides clear evidence of the significant role of self-assembly of hybrid nanofillers to produce a collaborative filler network and thus advanced rubber materials.

Appendix A. Supplementary data

Supplementary data include: loss modulus vs strain of NCs materials (Fig. S1); methods for the theoretical determination of ^{1}H mobility in NCs by Time Domain NMR; fitting of MSE and MSE/CPMG experiments for NR, SiO_2, Sep and mSep (Fig. S2); total hydrogen content for all pure

compounds (Table S1); contribution of each component to the hydrogen content of NCs (Table S2); and results of FID's analysis recorded for all pure compounds (Table S3).

Author contributions

Irene Tagliaro: Investigation, Data curation, Writing – originadraft, Writing - review & editing. Elkid Cobani: Investigation, Data curation. Elisa Carignani, Francesca Martini, Francesca Nardelli: Investigation, Data curation, Writing - review & editing. Lucia Conzatti, Paola Stagnaro: Investigation, Data curation, Formal analysis, Writing - review & editing. Massimiliano D'Arienzo, Luca Giannini, Roberto Scotti, Luciano Tadiello: Data curation, Formal analysis, Writing - review & editing. Barbara Di Credico: Conceptualization, Supervision; Validation; Visualization, Data curation, Formal analysis, Writing - original draft, Writing - review & editing.

Declaration of Competing Interest

The authors declare that they have no known competing financial interestsor personal relationships that could have appeared to influence the work reported in this paper.

Acknowledgements

I.T. thanks CORIMAV ("Consortium for the Research of Advanced Materials" between Pirelli and Milano Bicocca University) for its support within the PCAM European Doctoral Program.

F.N., E.C. and F.M. acknowledge Regione Toscana and Pirelli Tyre SpA for the financial support within POR FSE 2014-2020 Asse A - "NMR4DES" project. Silvia Borsacchi, Lucia Calucci and Marco Geppi are greatly acknowledged for helpful discussions.

References

Bokobza, L., 2006. Some new developments in rubber reinforcement. Compos. Interfaces 13, 345–354. https://doi.org/10.1163/156855406777408638

569 Bokobza, L., Leroy, E., Lalanne, V., 2009. Effect of filling mixtures of sepiolite and a surface
570 modified fumed silica on the mechanical and swelling behavior of a styrene-butadiene rubber.
571 Eur. Polym. J. 45, 996–1001. https://doi.org/10.1016/j.eurpolymj.2008.12.028
572 Borsacchi, S., Sudhakaran, U.P., Calucci, L., Martini, F., Carignani, E., Messori, M., Geppi, M.,
573 2018. Rubber-filler interactions in polyisoprene filled with in situ generated silica: A solid
574 state NMR study. Polymers (Basel). 10, 822.
575 https://doi.org/https://doi.org/10.3390/polym10080822
576 Carignani, E., Cobani, E., Martini, F., Nardelli, F., Borsacchi, S., Calucci, L., Di Credico, B.,
577 Tadiello, L., Giannini, L., Geppi, M., 2020. Effect of sepiolite treatments on the oxidation of
578 sepiolite/natural rubber nanocomposites prepared by latex compounding technique. Appl. Clay
579 Sci. 189, 105528. https://doi.org/doi:10.1016/j.clay.2020.105528
580 Cobani, E., 2018. Novel approach to rubber reinforcement by silica based nanofiller. University
581 Milano Bicocca. https://doi.org/http://hdl.handle.net/10281/199117
582 Cobani, E., Tagliaro, I., Geppi, M., Giannini, L., Leclère, P., Martini, F., Nguyen, T.C., Lazzaroni,
583 R., Scotti, R., Tadiello, L., 2019. Hybrid interface in sepiolite rubber nanocomposites: Role of
584 self-assembled nanostructure in controlling dissipative phenomena. Nanomaterials 9, 486.
585 https://doi.org/doi: 10.3390/nano9040486
586 D'Arienzo, M., Diré, S., Redaelli, M., Borovin, E., Callone, E., Di Credico, B., Morazzoni, F.,
587 Pegoretti, A., Scotti, R., 2018. Unveiling the hybrid interface in polymer nanocomposites
588 enclosing silsesquioxanes with tunable molecular structure: Spectroscopic, thermal and
589 mechanical properties. J. Colloid Interface Sci. 512, 609–617. https://doi.org/doi:
590 10.1016/j.jcis.2017.10.094
591 D'Arienzo, M., Redaelli, M., Callone, E., Conzatti, L., Di Credico, B., Dire, S., Giannini, L.,
592 Polizzi, S., Schizzi, I., Scotti, R., 2017. Hybrid SiO 2@ POSS nanofiller: a promising
593 reinforcing system for rubber nanocomposites. Mater. Chem. Front. 1, 1441–1452.
594 https://doi.org/doi: 10.1039/C7QM00045F

595 Das, A., Stöckelhuber, K.W., Rooj, S., Wang, D.-Y., Heinrich, G., 2010. Synergistic effects of
596 expanded nanoclay and carbon black on natural rubber compounds. Kautschuk Gummi
597 Kunststoffe 63, 296–302.
598 Di Credico, B., Cobani, E., Callone, E., Conzatti, L., Cristofori, D., D'Arienzo, M., Dirè, S.,
599 Giannini, L., Hanel, T., Scotti, R., Stagnaro, P., Tadiello, L., Morazzoni, F., 2018. Size-
600 controlled self-assembly of anisotropic sepiolite fibers in rubber nanocomposites. Appl. Clay
601 Sci. 152, 51–64. https://doi.org/10.1016/j.clay.2017.10.032
602 Di Credico, B., Tagliaro, I., Cobani, E., Conzatti, L., D'Arienzo, M., Giannini, L., Mascotto, S.,
603 Scotti, R., Stagnaro, P., Tadiello, L., 2019. A Green Approach for Preparing High-Loaded
604 Sepiolite/Polymer Biocomposites. Nanomaterials 9, 46. https://doi.org/10.3390/nano9010046
605 Feng, W., Tang, Z., Weng, P., Guo, B., 2015. Correlation of filler networking with reinforcement
606 and dynamic properties of SSBR/carbon black/silica composites. Rubber Chem. Technol. 88,
607 676–689. https://doi.org/doi:10.5254/rct.15.84881
608 Galimberti, M., Agnelli, S., Cipolletti, V., 2017a. Hybrid filler systems in rubber nanocomposites,
609 in: Sabu, T., Hanna, J.M. (Eds.), Progress in Rubber Nanocomposites. Woodhead Publishing,
610 Cambridge, pp. 349–414. https://doi.org/10.1016/B978-0-08-100409-8.00011-5
611 Galimberti, M., Cipolletti, V., Cioppa, S., Lostritto, A., Conzatti, L., 2017b. Reduction of filler
612 networking in silica based elastomeric nanocomposites with exfoliated organo-
613 montmorillonite. Appl. Clay Sci. 135, 168–175. https://doi.org/doi: 10.1016/j.clay.2016.09.017
614 Galimberti, M., Coombs, M., Cipolletti, V., Riccio, P., Riccò, T., Pandini, S., Conzatti, L., 2012.
615 Enhancement of mechanical reinforcement due to hybrid filler networking promoted by an
616 organoclay in hydrocarbon-based nanocomposites. Appl. Clay Sci. 65, 57–66.
617 https://doi.org/https://doi.org/10.1016/j.clay.2012.04.019
618 Giannini, L., Tadiello, L., Hanel, T., Cobani, E., Di Credico, B., D'Arienzo, M., Scotti, R.,
619 Morazzoni, F., Josè, P.C.J., Javier, J.S.D., 2018. Elastomeric materials for components of tyres
620 and tyres comprising modified silicate fibers. WO 2018078500, 03/05/2018.

621 Giannini, L., Tadiello, L., Hanel, T., Galimberti, M., Cipolletti, V., Peli, G., Morazzoni, F., Scotti,
622 R., Di Credico, B., 2016. Vulcanisable elastomeric materials for components of tyres
623 comprising modified silicate fibers, and tyres thereof. WO2016174629 10,308,072, 2019.
624 Locatelli, D., Pavlovic, N., Barbera, V., Giannini, L., Galimberti, M., 2020. Sepiolite as reinforcing
625 filler for rubber composites: From the chemical compatibilization to the commercial
626 exploitation. KGK Kautschuk Gummi Kunststoffe 73, 26–35.
627 Matsui, S., 1991. Solid-state NMR imaging by magic sandwich echoes. Chem. Phys. Lett. 179,
628 187–190. https://doi.org/https://doi.org/10.1016/0009-2614(91)90313-X
629 Meiboom, S., Gill, D., 1958. Modified spin-echo method for measuring nuclear relaxation times.
630 Rev. Sci. Instrum. 29, 688–691. https://doi.org/https://doi.org/10.1063/1.1716296
631 Mohanty, T.R., Neeraj, P.K.., Ramakrishnan, S.., Amarnath, S.K.P., Lorenzetti, D., Mohamed, P..,
632 2021. Sepiolite nanoclay as a reinforcing filler in the NR/BR matrix. RubberWorld.
633 Mora-Barrantes, I., Ibarra, L., Rodríguez, A., Gonzalez, L., Valentín, J.L., 2011. Elastomer
634 composites based on improved fumed silica and carbon black. Advantages of mixed
635 reinforcing systems. J. Mater. Chem. 21, 17526–17533.
636 https://doi.org/doi:10.1039/C1JM12106E
637 Mostoni, S., Milana, P., Di Credico, B., D'Arienzo, M., Scotti, R., 2019. Zinc-based curing
638 activators: new trends for reducing zinc content in rubber vulcanization process. Catalysts 9,
639 664. https://doi.org/doi: 10.3390/catal9080664
640 O'Brien, J., Cashell, E., Wardell, G.., McBrierty, V., 1976. An NMR investigation of the interaction
641 between carbon black and cis-polybutadiene. Macromolecules 9, p653.
642 https://doi.org/https://doi.org/10.1021/ma60052a025
643 Ou, Y., Yu, Z., Vidal, A., Donnet, J.B., 1996. Effects of alkylation of silicas on interfacial
644 interaction and molecular motions between silicas and rubbers. J. Appl. Polym. Sci. 59, 1321–
645 1328. https://doi.org/https://doi.org/10.1002/(SICI)1097-4628(19960222)59:8<1321::AID-
646 APP16>3.0.CO;2-8

Redaelli, M., D'Arienzo, M., Brus, J., Di Credico, B., Geppi, M., Giannini, L., Matejka, L., Martini, F., Panattoni, F., Spirkova, M., 2018. On the key role of SiO2@ POSS hybrid filler in tailoring networking and interfaces in rubber nanocomposites. Polym. Test. 65, 429–439. https://doi.org/https://doi.org/10.1016/j.polymertesting.2017.12.022

Rhim, W.-K., Pines, A., Waugh, J.S., 1971. Time-reversal experiments in dipolar-coupled spin systems. Phys. Rev. B 3, 684. https://doi.org/https://doi.org/10.1103/PhysRevB.3.684

Sattayanurak, S., Noordermeer, J.W.M., Sahakaro, K., Kaewsakul, W., Dierkes, W.K., Blume, A., 2019. Silica-reinforced natural rubber: synergistic effects by addition of small amounts of secondary fillers to silica-reinforced natural rubber tire tread compounds. Adv. Mater. Sci. Eng. https://doi.org/doi.org/10.1155/2019/5891051

Scotti, R., Conzatti, L., D'Arienzo, M., Di Credico, B., Giannini, L., Hanel, T., Stagnaro, P., Susanna, A., Tadiello, L., Morazzoni, F., 2014. Shape controlled spherical (0D) and rod-like (1D) silica nanoparticles in silica/styrene butadiene rubber nanocomposites: Role of the particle morphology on the filler reinforcing effect. Polymer (Guildf). 55, 1497–1506. https://doi.org/https://doi.org/10.1016/j.polymer.2014.01.025

Scotti, R., D'Arienzo, M., Di Credico, B., Giannini, L., Morazzoni, F., 2018. Silica–Polymer Interface and Mechanical Reinforcement in Rubber Nanocomposites, in: Delville, M.-H., Taubert, A. (Eds.), Hybrid Organic-Inorganic Interfaces: Towards Advanced Functional Materials. Wiley Online Library, Hoboken, pp. 151–198. https://doi.org/https://doi.org/10.1002/9783527807130.ch4

Senthilvel, K., Vishvanathperumal, S., Prabu, B., John Baruch, L., 2016. Studies on the morphology, cure characteristics and mechanical properties of acrylonitrile butadiene rubber with hybrid filler (carbon black/silica) composite. Polym. Polym. Compos. 24, 473–480. https://doi.org/https://doi.org/10.1177/096739111602400705

Staropoli, M., Rogé, V., Moretto, E., Didierjean, J., Michel, M., Duez, B., Steiner, P., Thielen, G., Lenoble, D., Thomann, J.S., 2021. Hybrid silica-based fillers in nanocomposites: Influence of

673 isotropic/isotropic and isotropic/anisotropic fillers on mechanical properties of styrene-
674 butadiene (SBR)-based rubber. Polymers (Basel). 13. https://doi.org/10.3390/polym13152413
675 Susanna, A., D'Arienzo, M., Di Credico, B., Giannini, L., Hanel, T., Grandori, R., Morazzoni, F.,
676 Mostoni, S., Santambrogio, C., Scotti, R., 2017. Catalytic effect of ZnO anchored silica
677 nanoparticles on rubber vulcanization and cross-link formation. Eur. Polym. J. 93, 63–74.
678 https://doi.org/10.1016/j.eurpolymj.2017.05.029
679 Tadiello, L., Cipolletti, V.R., Giannini, L., Hanel, T., Galimberti, M., Scotti, R., Di Credico, B.,
680 Morazzoni, F., D'arienzo, M., Tagliaro, I., 2018. Elastomeric compositions comprising silicate
681 fibres with needle-shaped morphology of nanometric size and tyres for vehicles that comprise
682 them. WO2018116125 16/469,849, 2020.
683 Tadiello, L., D'Arienzo, M., Di Credico, B., Hanel, T., Matejka, L., Mauri, M., Morazzoni, F.,
684 Simonutti, R., Spirkova, M., Scotti, R., 2015. The filler-rubber interface in styrene butadiene
685 nanocomposites with anisotropic silica particles: Morphology and dynamic properties. Soft
686 Matter 11, 4022–4033. https://doi.org/10.1039/c5sm00536a
687 Tagliaro, I., Di Credico, B., Moncho-Jordá, A., 2020. Electrostatic depletion effects on the stability
688 of colloidal dispersions of sepiolite and natural rubber latex. J. Colloid Interface Sci. 560, 606–
689 617. https://doi.org/https://doi.org/10.1016/j.jcis.2019.10.083
690 Tripaldi, L., Callone, E., D'Arienzo, M., Dirè, S., Giannini, L., Mascotto, S., Meyer, A., Scotti, R.,
691 Tadiello, L., Di Credico, B., 2021. Silica hairy nanoparticles: a promising material for self-
692 assembling processes. Soft Matter 29–31. https://doi.org/10.1039/d1sm01085a
693 Uhrlandt, S., Blume, A., 2001. Silica in green tyres-processes, products, properties. Kautschuk
694 Gummi Kunststoffe 54, 520.
695 Wang, L., Zhao, S., 2010. Study on the structure-mechanical properties relationship and antistatic
696 characteristics of SSBR composites filled with SiO2/CB. J. Appl. Polym. Sci. 118, 338–345.
697 https://doi.org/https://doi.org/10.1002/app.32372
698